Exploring the physical origin of blazar flares with a time-dependent one-zone model

P. Thevenet, A. Zech, C. Boisson
LUTh - Observatoire de Paris, PSL Université,
Université Paris Cité, CNRS

Workshop on Numerical Multi-Messenger Modeling
APC Laboratory, February 22nd 2024

Introduction: blazar emission variability

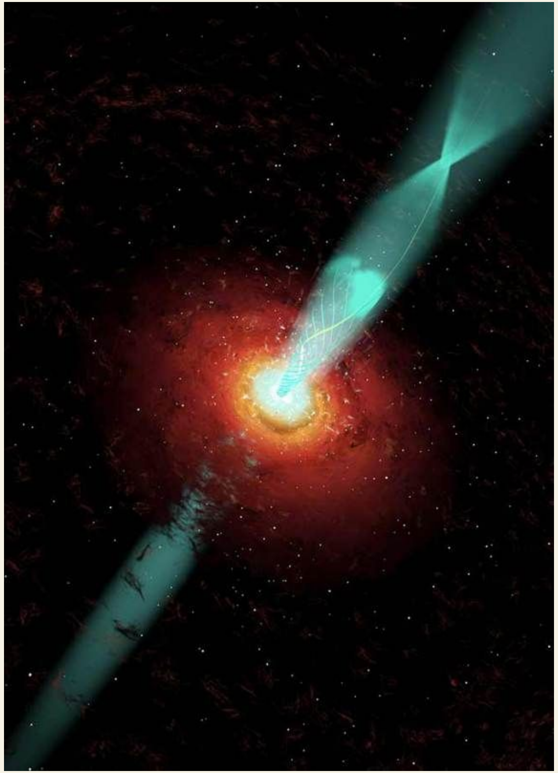

Credit: Marscher et al., Wolfgang Steffen, NRAO/AUI/NSF

γ-rays
X-rays
Optical
Radio

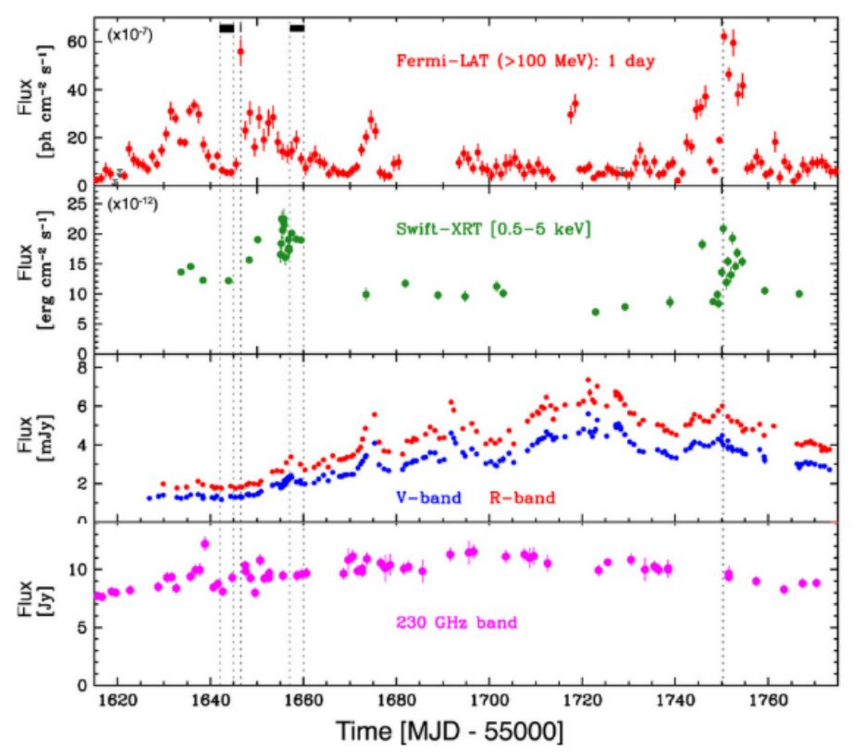

Example of multiwavelength (MWL) light curves of 3C 279 covering the 2013–2014 active period. Adapted from Hayashida et al. 2015

Introduction: blazar emission variability

Problem: lack of a general picture of the physical origin of blazar flares

Objective: simulate isolated short-term blazar flares from different scenarios with a **leptonic single-zone SSC model** and identify characteristic signatures in the light curves

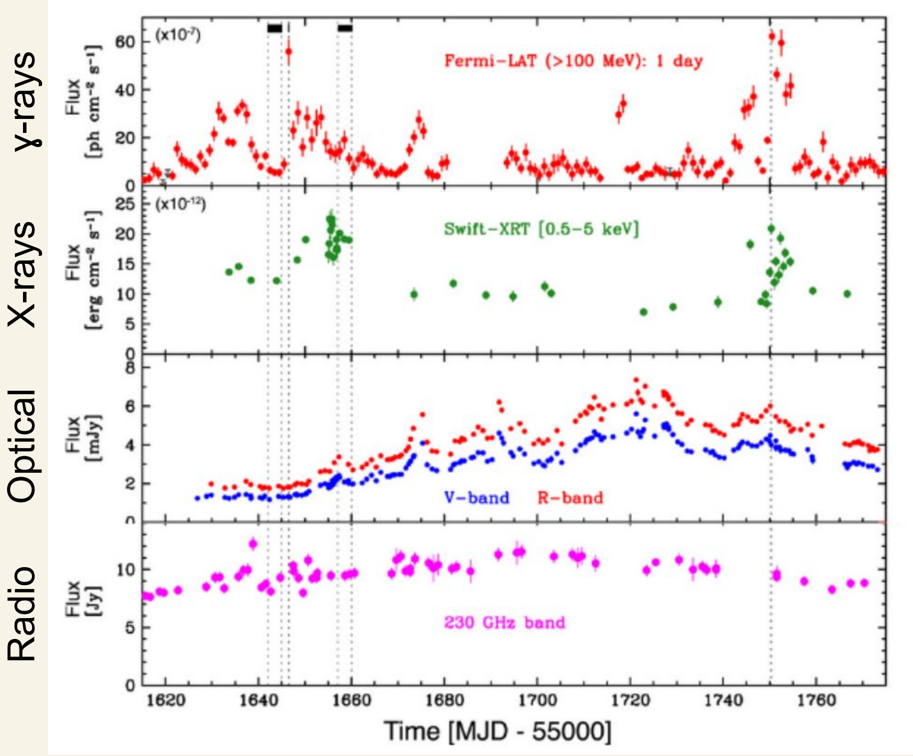

Example of multiwavelength (MWL) light curves of 3C 279 covering the 2013–2014 active period. Adapted from Hayashida et al. 2015

Introduction: blazar emission variability

Problem: lack of a general picture of the physical origin of blazar flares

Objective: simulate isolated short-term blazar flares from different scenarios with a **leptonic single-zone SSC model** and identify characteristic signatures in the light curves

- Systematic study of particle injection/acceleration flares

- Comparison of different scenarios

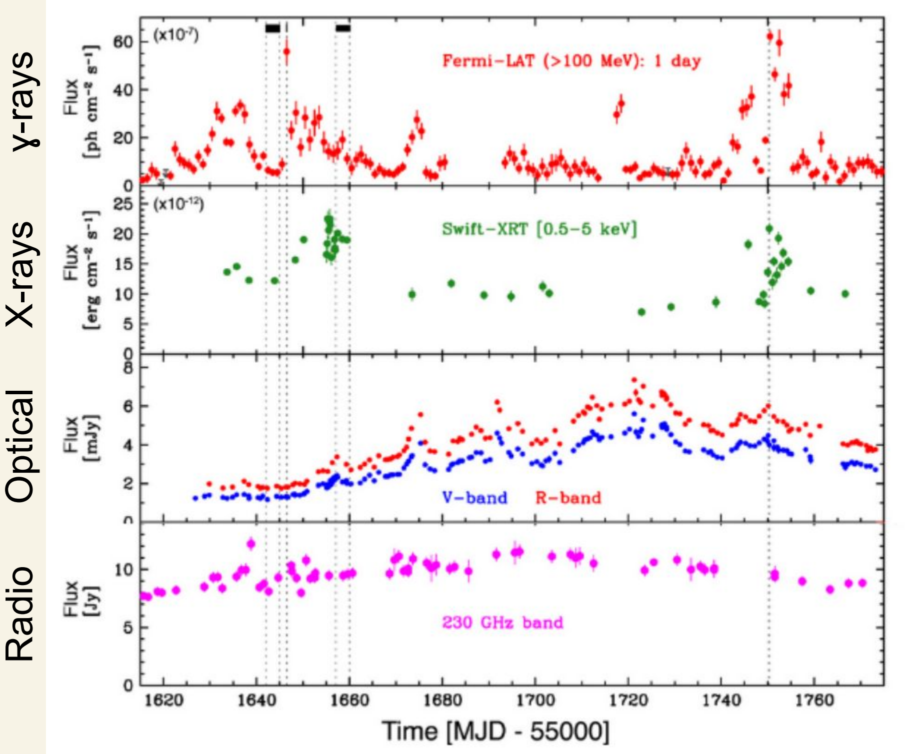

Example of multiwavelength (MWL) light curves of 3C 279 covering the 2013–2014 active period. Adapted from Hayashida et al. 2015

1. Radiative model

Fokker-Planck equation solved in the EMBLEM code, Dmytriiev et al. (2021):

Cooling terms

Acceleration terms

$$\frac{\partial N_e(\gamma,t)}{\partial t} = \frac{\partial}{\partial \gamma}\left[\left(b_c(\gamma,t)\gamma^2 + \frac{1}{t_{ad}}\gamma - a(t)\gamma - \frac{2}{\gamma}D_{F_{II}}(\gamma,t)\right)N_e(\gamma,t)\right] + \frac{\partial}{\partial \gamma}\left(D_{F_{II}}(\gamma,t)\frac{\partial N_e(\gamma,t)}{\partial \gamma}\right) - N_e(\gamma,t)\left(\frac{1}{t_{esc}} + \frac{3}{t_{ad}}\right) + Q_{inj}(\gamma,t)$$

Injection term

1. Radiative model

Fokker-Planck equation solved in the EMBLEM code, Dmytriiev et al. (2021):

Cooling terms — Acceleration terms

$$\frac{\partial N_e(\gamma,t)}{\partial t} = \frac{\partial}{\partial \gamma}\left[\left(b_c(\gamma,t)\gamma^2 + \frac{1}{t_{ad}}\gamma - a(t)\gamma - \frac{2}{\gamma}D_{F_{II}}(\gamma,t)\right)N_e(\gamma,t)\right] + \frac{\partial}{\partial \gamma}\left(D_{F_{II}}(\gamma,t)\frac{\partial N_e(\gamma,t)}{\partial \gamma}\right) - N_e(\gamma,t)\left(\frac{1}{t_{esc}} + \frac{3}{t_{ad}}\right) + Q_{inj}(\gamma,t)$$

Injection term

<u>Cooling</u>

- Synchrotron and Inverse Compton: $b_c(\gamma,t)$
- Adiabatic expansion: $t_{ad}(t) = \frac{R(t)}{\beta_{exp}c}$
- Escape: $t_{esc}^{(turb)} = \left(\frac{R_t}{c}\right)^2 \left(\frac{\delta B}{B}\right)^2 \frac{c}{\lambda_{max}} \left(\frac{r_L}{\lambda_{max}}\right)^{q-2}$

<u>Acceleration</u>

- Fermi I: injection with time-dependent maximum Lorentz factor
- Fermi II: $D_{F_{II}}(\gamma,t) = \frac{p^2}{t_{F_{II}}}$

$$t_{F_{II}} = \frac{1}{\beta_A^2}\left(\frac{\delta B}{B}\right)^{-2} \frac{\lambda_{max}}{c} \left(\frac{r_L}{\lambda_{max}}\right)^{2-q}$$

2. Scenarios studied

Quiescent steady-state injection:

$$Q_{inj}(\gamma) = N_{inj}\left(\frac{\gamma}{\gamma_{inj,pivot}}\right)^{\alpha_{inj}} \exp\left(-\frac{\gamma}{\gamma_{inj,cut}}\right)$$

Parameter	Variable	Value	Unit
	Source		
Initial magnetic field	B_0	0.04	Gauss
Initial blob radius	R_0	2.8e16	cm
Blob Doppler factor	δ	29	-
Redshift	z	0.0308	-
	Continuous injection spectrum		
Spectrum normalization	N_{inj}	1.86e-14	$cm^{-3}s^{-1}$
Spectrum slope	α_{inj}	-2.23	-
Pivot Lorentz factor	$\gamma_{inj,pivot}$	1.0e5	-
Cutoff Lorentz factor	$\gamma_{inj,cut}$	5.8e5	-
Minimal injected Lorentz factor	$\gamma_{inj,min}$	800	-

Parameters based on the study of Mrk421, Dmytriiev et al. (2021)

2. Scenarios studied

Quiescent steady-state injection:

$$Q_{inj}(\gamma) = N_{inj} \left(\frac{\gamma}{\gamma_{inj,pivot}} \right)^{\alpha_{inj}} \exp\left(-\frac{\gamma}{\gamma_{inj,cut}} \right)$$

Parameter	Variable	Value	Unit
	Source		
Initial magnetic field	B_0	0.04	Gauss
Initial blob radius	R_0	2.8e16	cm
Blob Doppler factor	δ	29	-
Redshift	z	0.0308	-
	Continuous injection spectrum		
Spectrum normalization	N_{inj}	1.86e-14	$cm^{-3}s^{-1}$
Spectrum slope	α_{inj}	-2.23	-
Pivot Lorentz factor	$\gamma_{inj,pivot}$	1.0e5	-
Cutoff Lorentz factor	$\gamma_{inj,cut}$	5.8e5	-
Minimal injected Lorentz factor	$\gamma_{inj,min}$	800	-

Parameters based on the study of Mrk421, Dmytriiev et al. (2021)

Flares resulting from a perturbation of the steady-state:

- Simple particle injection
- Particle injection and adiabatic expansion
- Diffusive shock acceleration (Fermi I)
- Stochastic acceleration (Fermi II)

2. Scenarios studied: simple particle injection

Power law with exponential cutoff:

$$Q_{add}(\gamma) = \boxed{N_{add}} \left(\frac{\gamma}{\gamma_{add,pivot}} \right)^{\alpha_{add}} \exp\left(-\frac{\gamma}{\gamma_{add,cut}} \right)$$

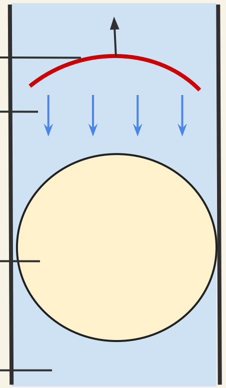

Sketch of a one-zone flaring scenario by particle injection

→ We vary the additional injection rate

Flaring injection spectrum			
Spectrum slope	α_{add}	-2.23	-
Pivot Lorentz factor	$\gamma_{add,pivot}$	1.0e5	-
Cutoff Lorentz factor	$\gamma_{add,cut}$	5.8e5	-
Minimal injected Lorentz factor	$\gamma_{add,min}$	800	-

Parameters of the flaring injection phase

2. Scenarios studied: simple particle injection

Electron Distribution

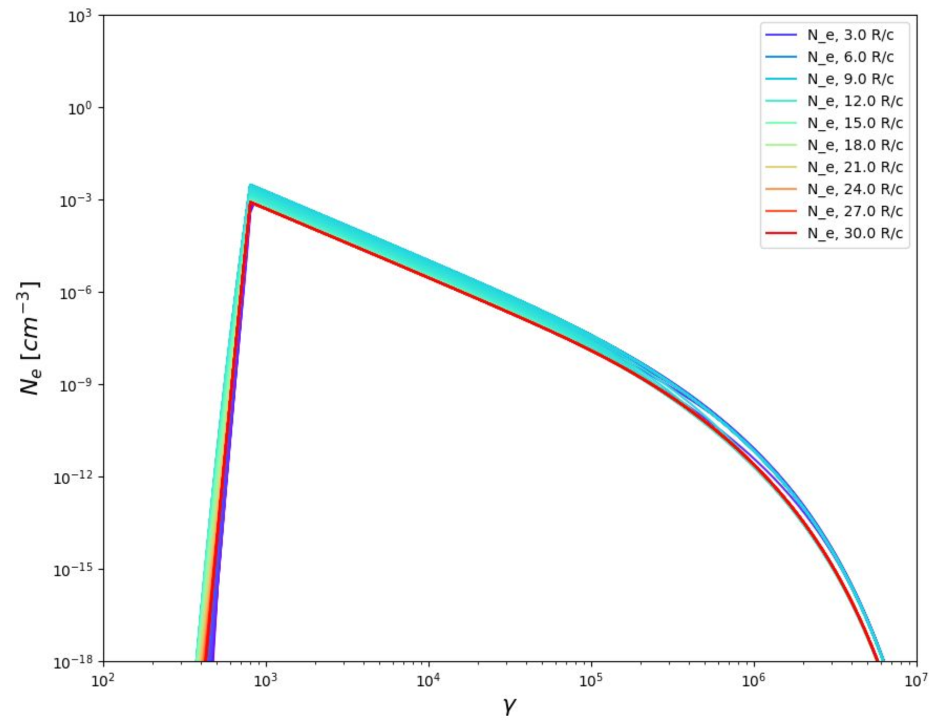

Spectral Energy Distribution (SED)

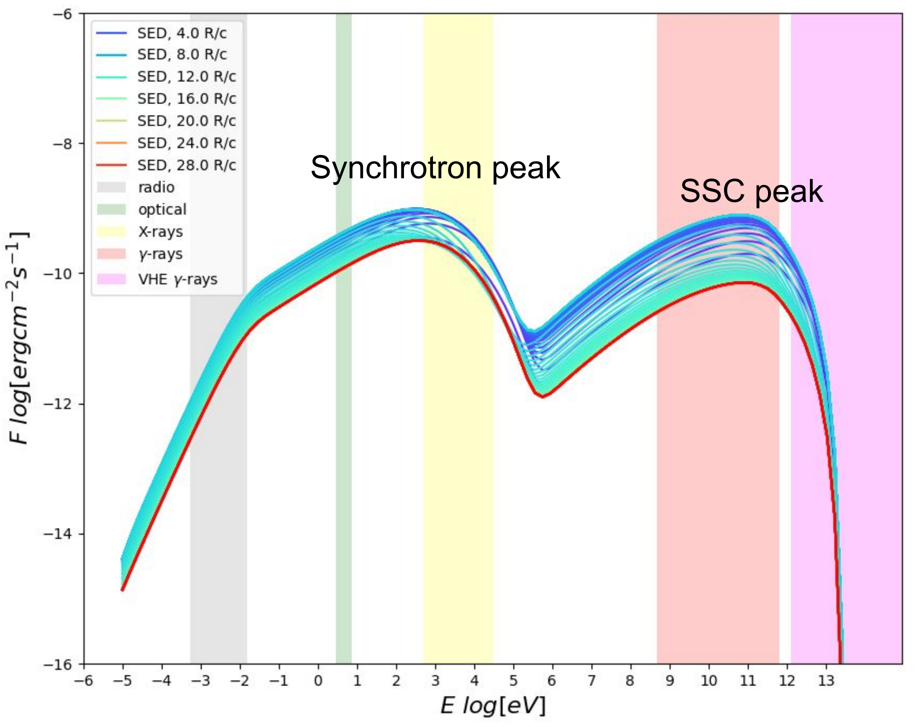

2. Scenarios studied: simple particle injection

Optical

X-rays

γ-rays

VHE γ-rays

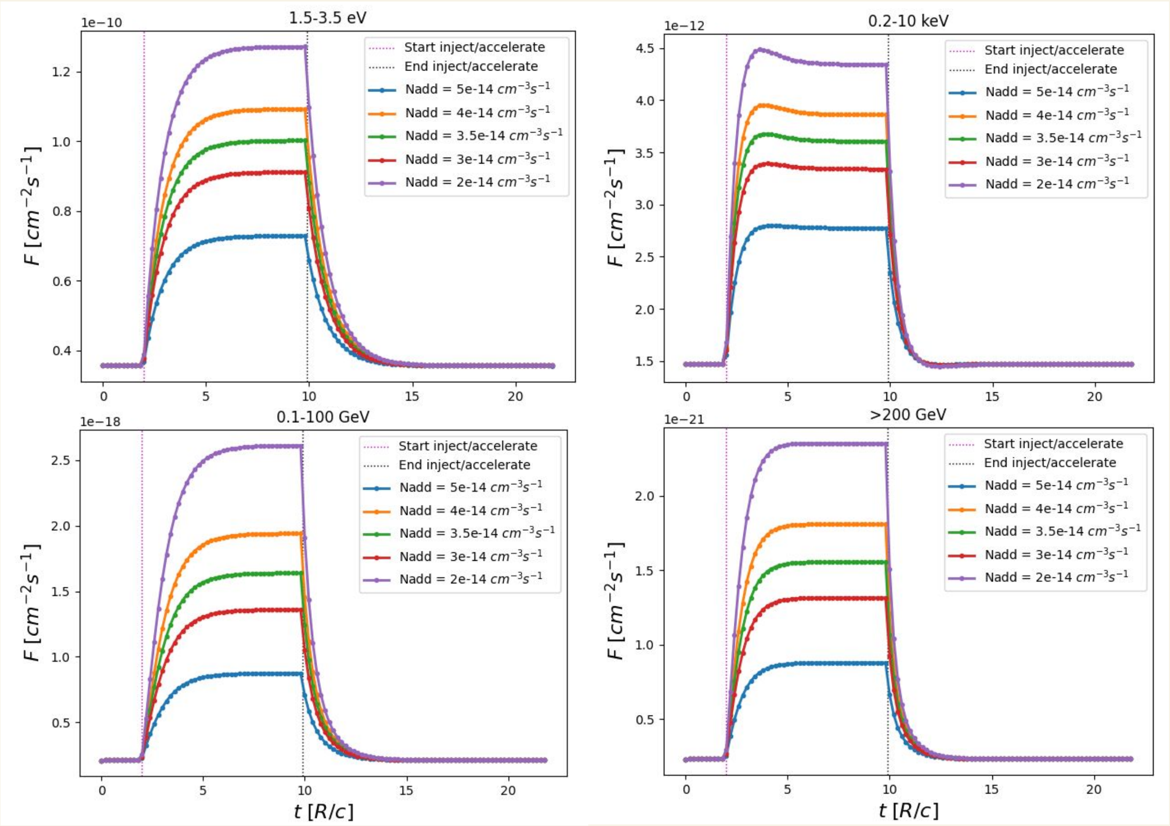

2. Scenarios studied: injection and adiabatic expansion

Power law with exponential cutoff: $$Q_{add}(\gamma) = N_{add} \left(\frac{\gamma}{\gamma_{add,pivot}} \right)^{\alpha_{add}} \exp\left(-\frac{\gamma}{\gamma_{add,cut}} \right)$$

Intrinsic opening angle of the jet leading to the blob’s adiabatic expansion, Tramacere et al. (2022):

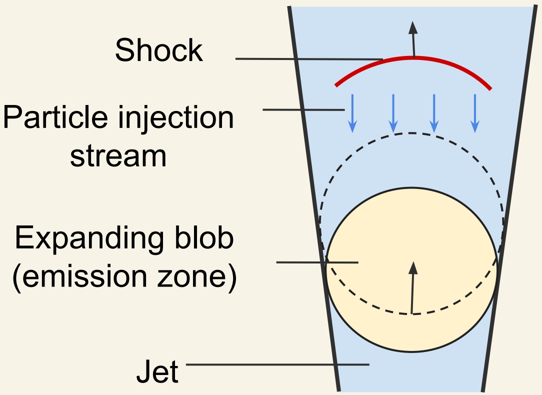

Sketch of a one-zone flaring scenario by particle injection with adiabatic expansion

$$t_{ad}(t) = \frac{R(t)}{\beta_{exp} c}$$

$$\beta_{exp} = \beta_{jet} \tan(\alpha)$$

Opening angle from best-fit value ρ≃0.26 rad based on VLBI observations, Pushkarev et al. (2009)

$$\alpha = \rho / \Gamma$$

Chosen opening angle: α≃0.44°

→ We vary the additional injection rate

2. Scenarios studied: injection and adiabatic expansion

Optical

X-rays

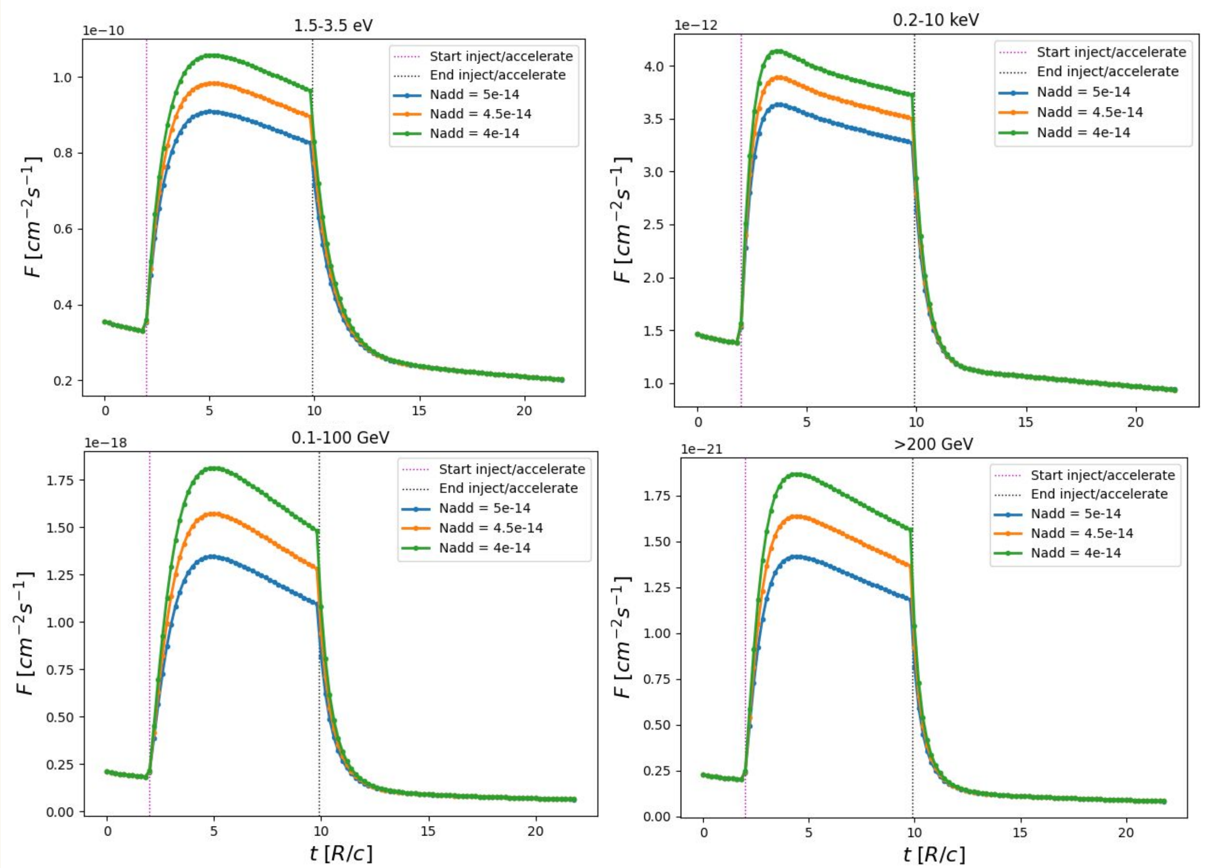

γ-rays

VHE γ-rays

2. Scenarios studied: Fermi I acceleration

Equivalent to an additional injection, Kirk et al. (1998):

- Power law with exponential cutoff
- Time-dependent cutoff and maximum Lorentz factor

$$Q_{add}(\gamma) = N_{add}\left(\frac{\gamma}{\gamma_{add,pivot}}\right)^{\alpha_{add}} \exp\left(-\frac{\gamma}{\gamma_{add,cut}}\right)$$

$$\gamma_{add,cut} = \left[\frac{1}{t_{max}} + \left(\frac{1}{\gamma_{add,min}} - \frac{1}{\gamma_{max}}\right) e^{-t/t_{shock}}\right]^{-1}$$

$$\gamma_{max} = (\beta_s t_{shock})^{-1}$$

$$\beta_s = \frac{4\sigma_T}{3m_e c}\left(\frac{B^2}{2\mu_0}\right)$$

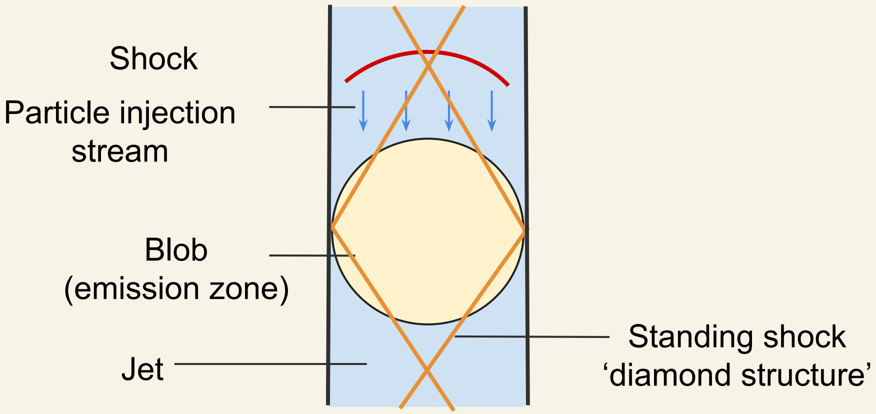

Sketch of a one-zone flaring scenario by Fermi I acceleration

→ Fixed injection rate
→ We vary the shock timescale

2. Scenarios studied: Fermi I acceleration

Optical

X-rays

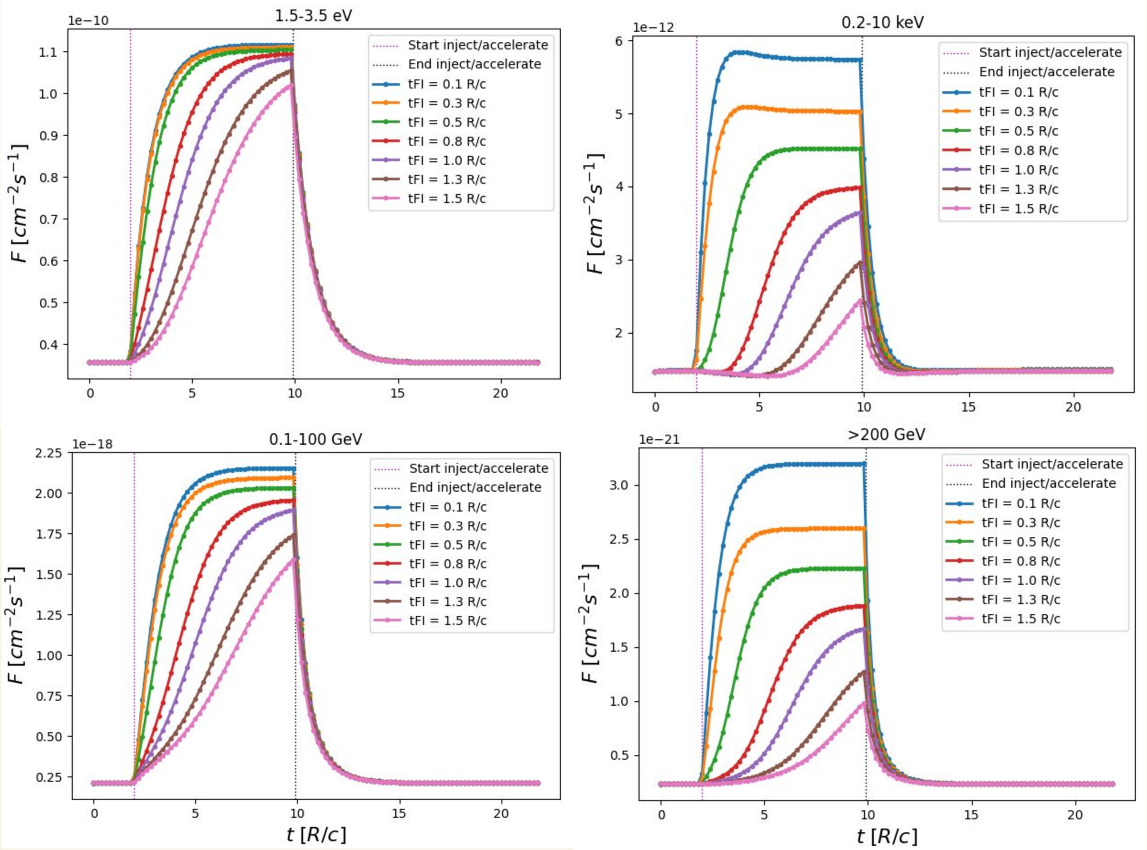

γ-rays

VHE γ-rays

⇒ Different rise and plateau times, shift in peak maximum with the acceleration timescale

2. Scenarios studied: Fermi II acceleration

We study three turbulence regimes:

- Hard-sphere: q=2
- Kolmogorov: q=5/3
- Kraichnan: q=3/2

Escape timescale

$$t_{esc}^{(turb)} = \left(\frac{R_t}{c}\right)^2 \left(\frac{\delta B}{B}\right)^2 \frac{c}{\lambda_{max}} \left(\frac{r_L}{\lambda_{max}}\right)^{q-2}$$

Acceleration timescale

$$t_{F_{II}} = \frac{1}{\beta_A^2} \left(\frac{\delta B}{B}\right)^{-2} \frac{\lambda_{max}}{c} \left(\frac{r_L}{\lambda_{max}}\right)^{2-q}$$

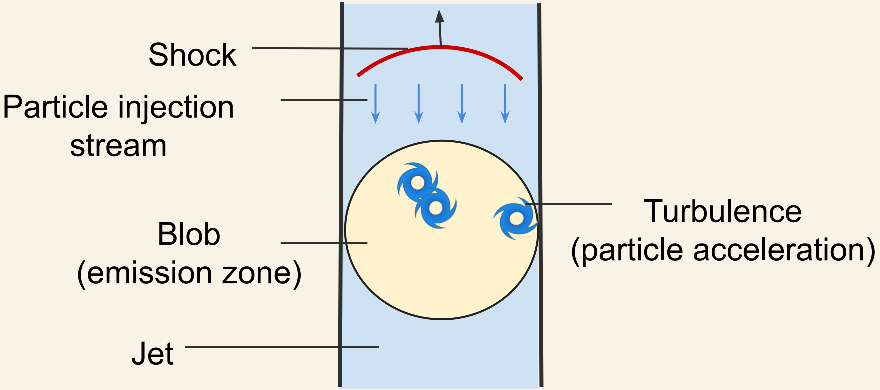

Sketch of a one-zone flaring scenario by Fermi II acceleration

Constraints on the parameters:

$$r_L < \lambda_{max} < R$$

$$0 < \frac{\delta B}{B} < 1$$

2. Scenarios studied: hard-sphere Fermi II acceleration

Optical

X-rays

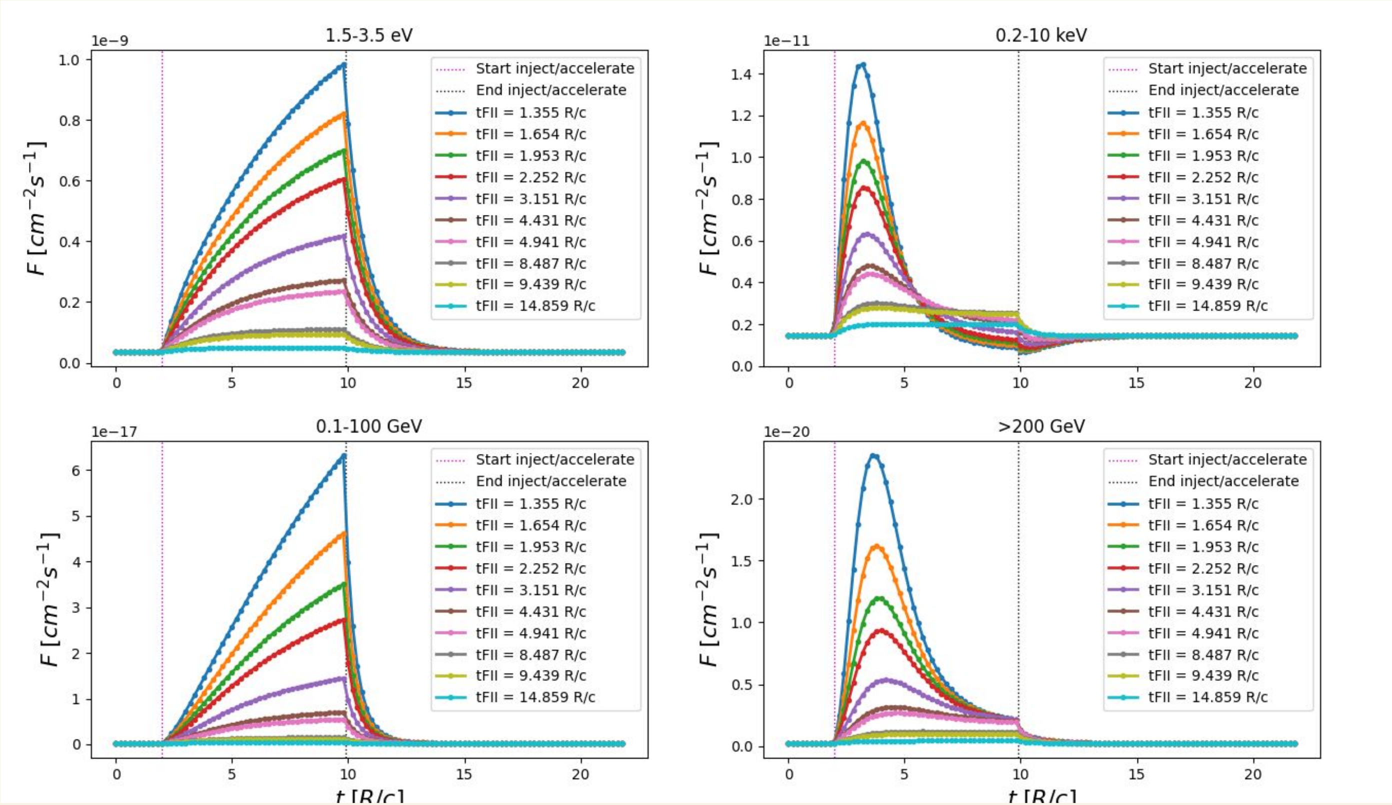

γ-rays

VHE γ-rays

⇒ Shift of the peak maximum and peak time with the acceleration timescale

3. Comparison: Fermi I and Fermi II acceleration

Optical

X-rays

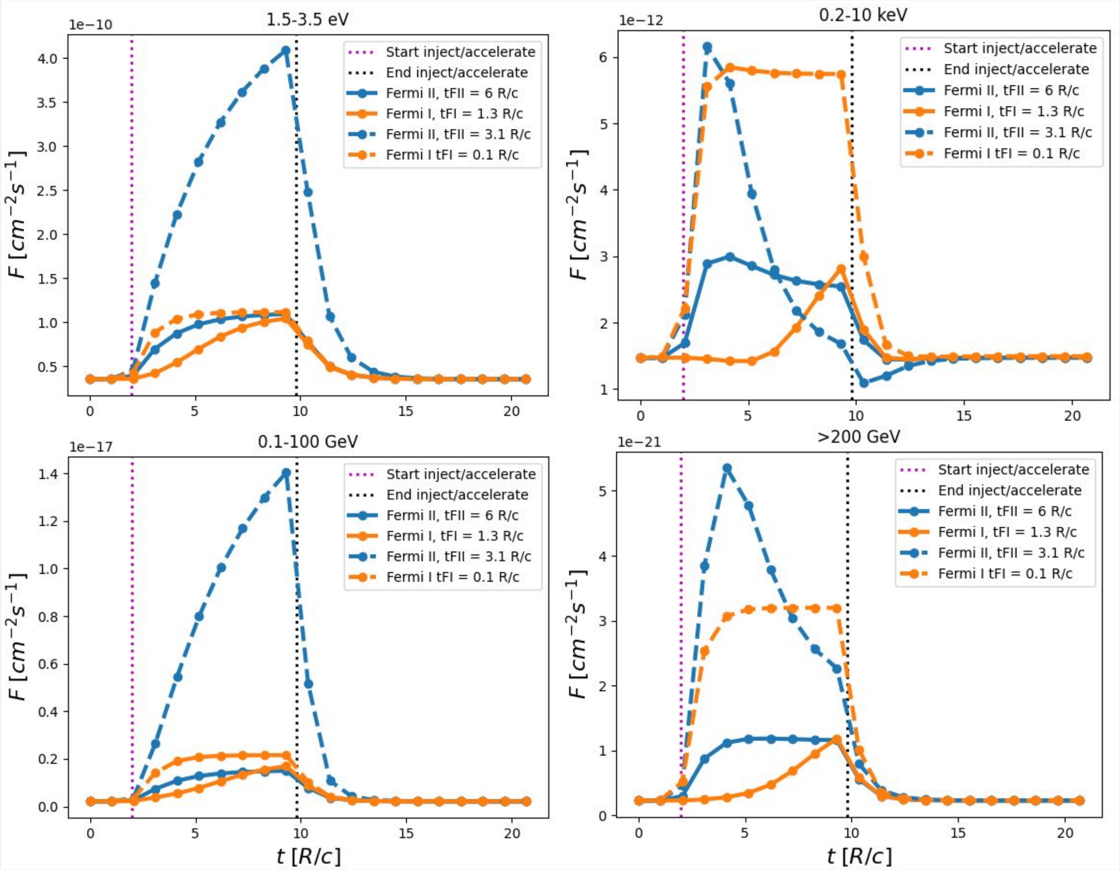

γ-rays

VHE γ-rays

⇒ Differences in asymmetry, variability amplitude, rise and plateau times

3. Comparison: all four scenarios

Optical

X-rays

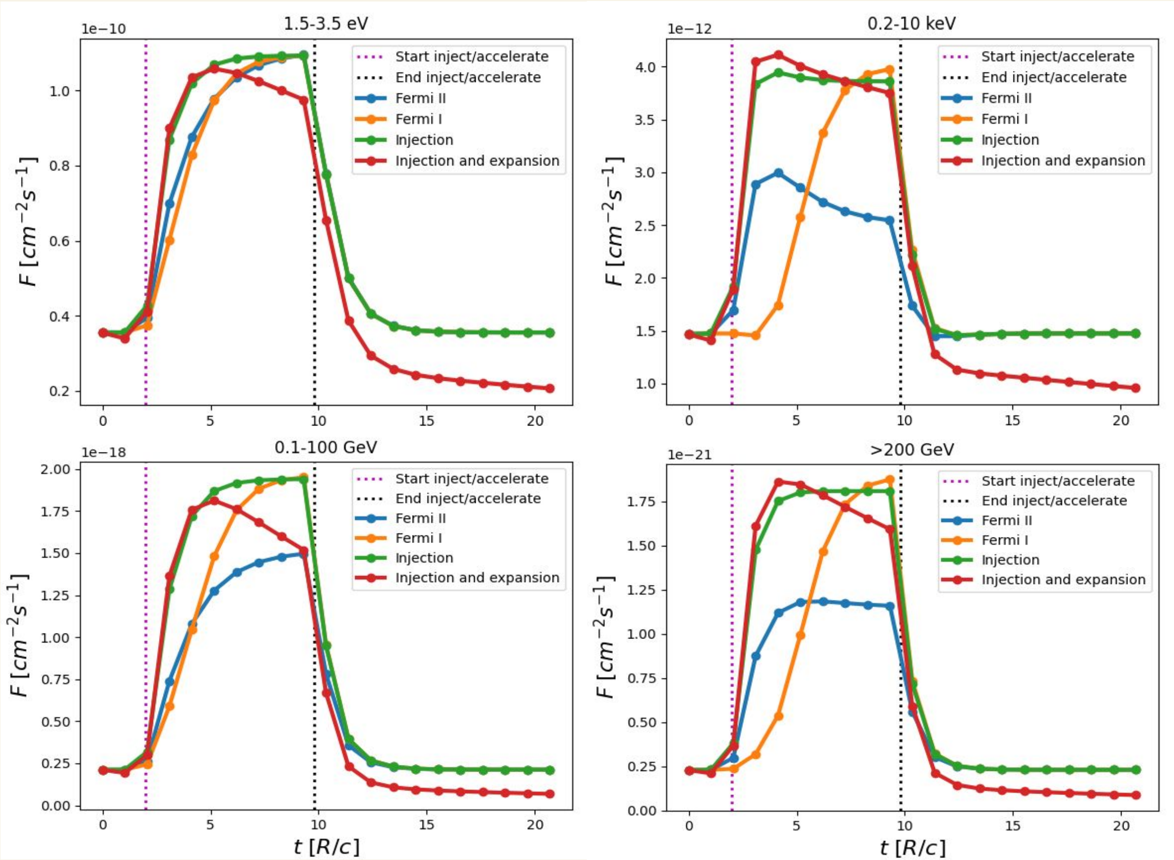

γ-rays

VHE γ-rays

⇒ Differences in asymmetry, plateau reaching time, variability amplitude

Conclusion

- Recognizable patterns between flares by injection, injection and expansion, Fermi I and Fermi II acceleration using different energy bands:
  Rise time, relative variability amplitude, asymmetry, possible plateau phases

- Short timescale Fermi II flares → high Compton dominance flares described without external photon field

- Kolmogorov and Kraichnan turbulence: same flare shapes as in the high Compton dominance hard-sphere regime

Conclusion

- Recognizable patterns between flares by injection, injection and expansion, Fermi I and Fermi II acceleration using different energy bands:
  Rise time, relative variability amplitude, asymmetry, possible plateau phases

- Short timescale Fermi II flares → high Compton dominance flares described without external photon field

- Kolmogorov and Kraichnan turbulence: same flare shapes as in the high Compton dominance hard-sphere regime

Outlook:

- Compare the observed behaviour with SEDs in the Thomson regime
- Determine a method to constrain the emission mechanism of observed MWL rapid flares
- Simulate LCs including external photon fields

Extra slides

2. Extra - Different flaring spectrum injection

Electron Distribution

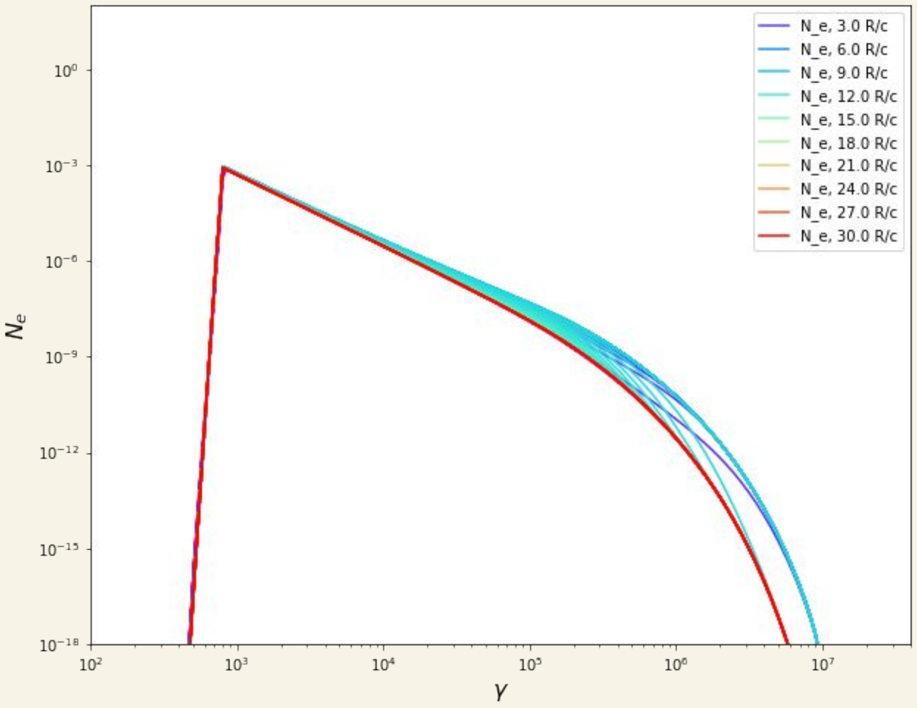

Spectral Energy Distribution (SED)

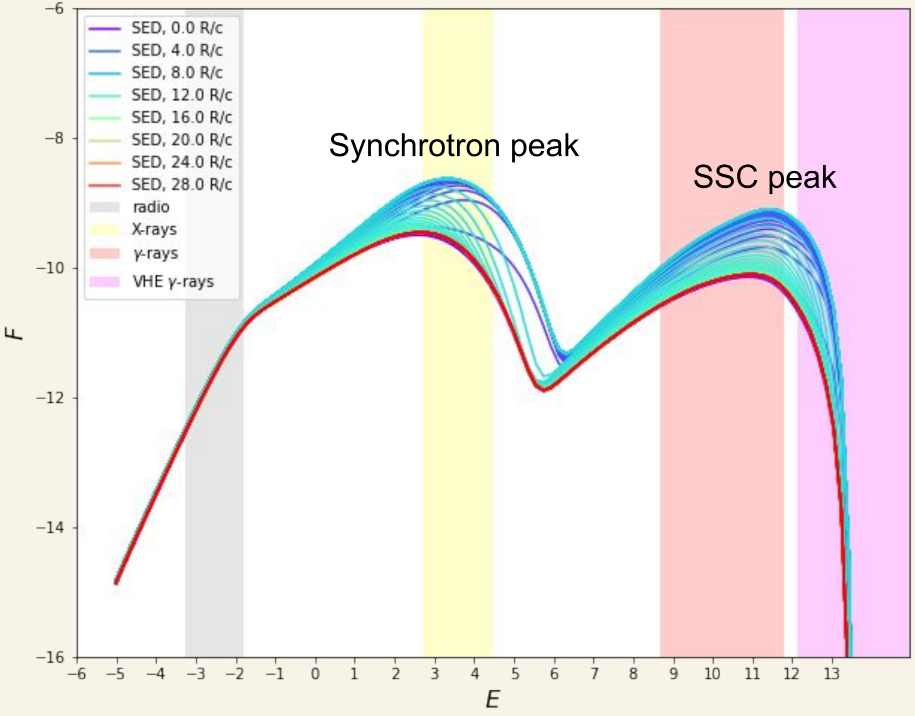

Extra - Particle injection

Compton dominance: ratio of the flux at the IC peak to the flux at the Synchrotron peak

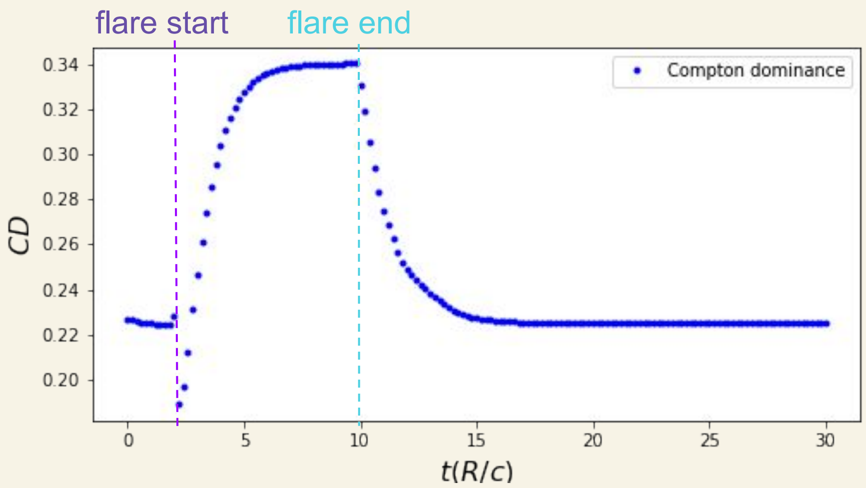

Spectral Energy Distribution

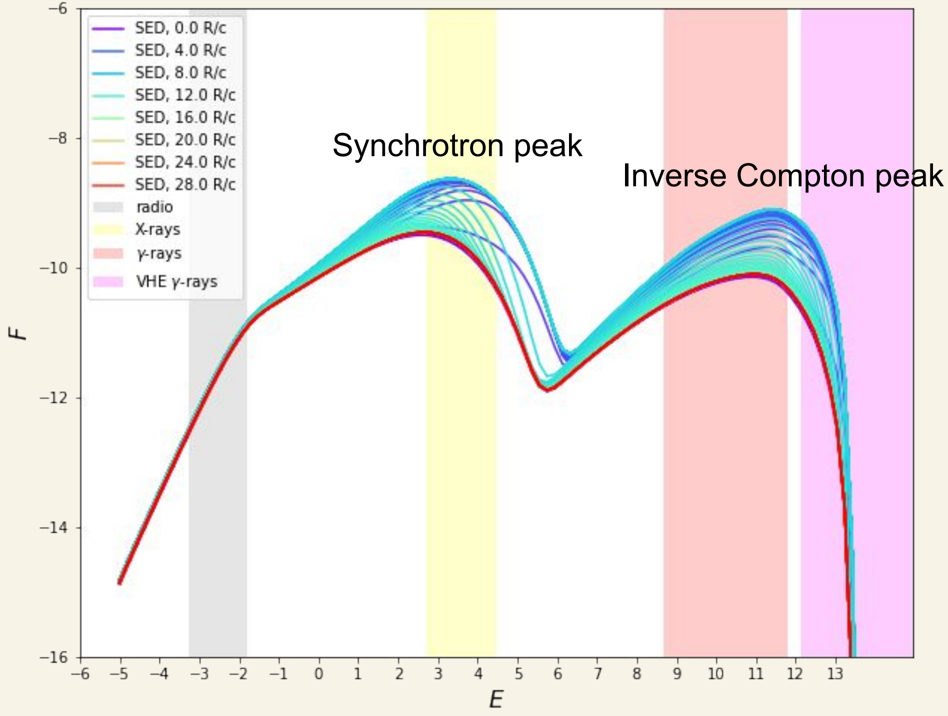

Extra - Injection with adiabatic expansion

Electron Distribution

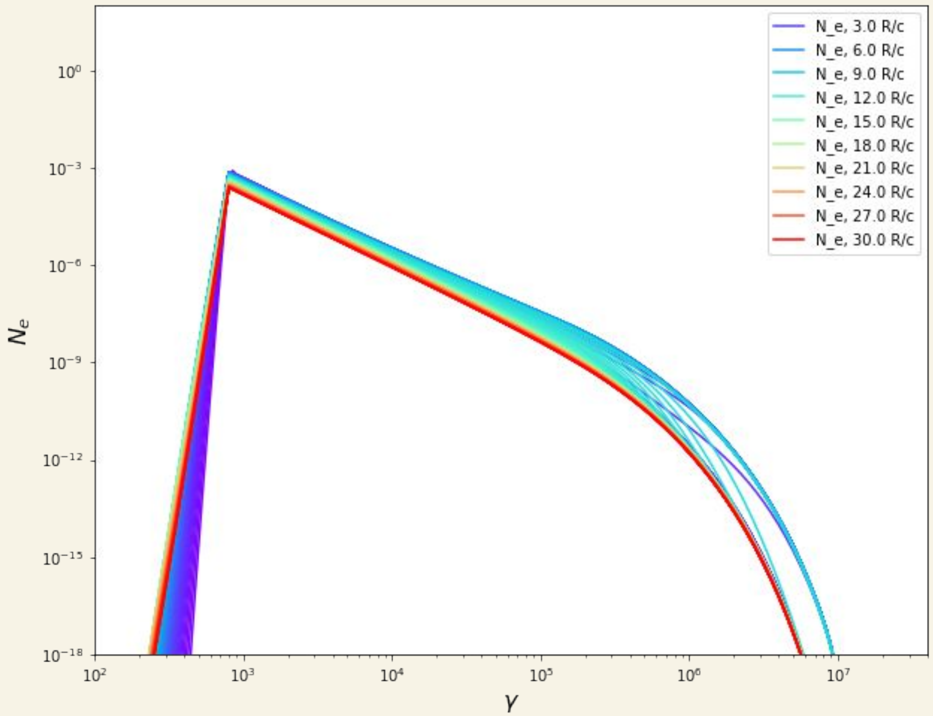

Spectral Energy Distribution

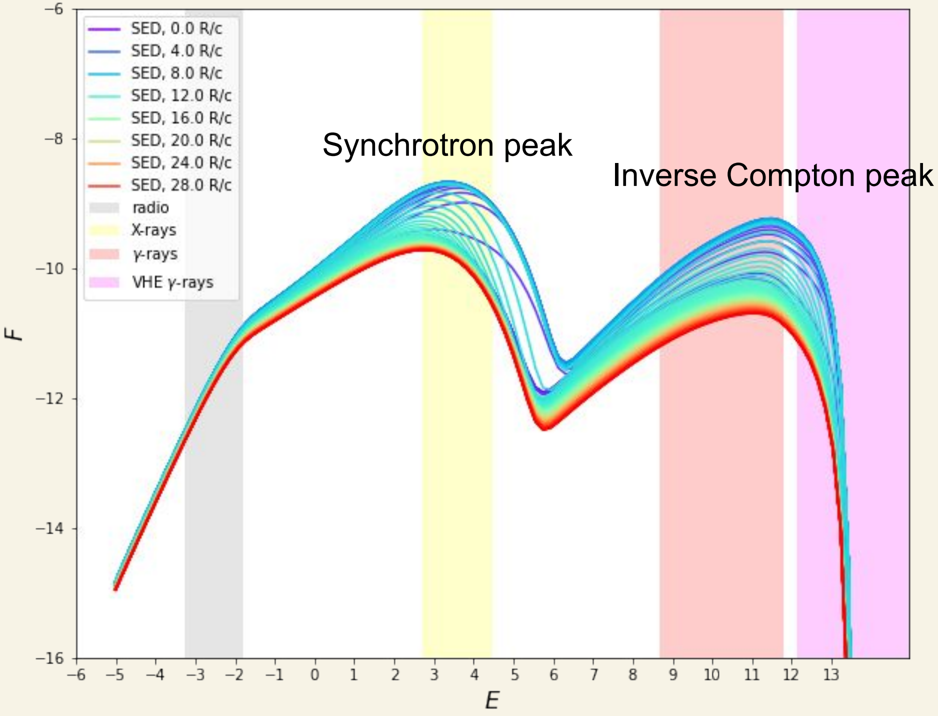

Extra - Injection with adiabatic expansion

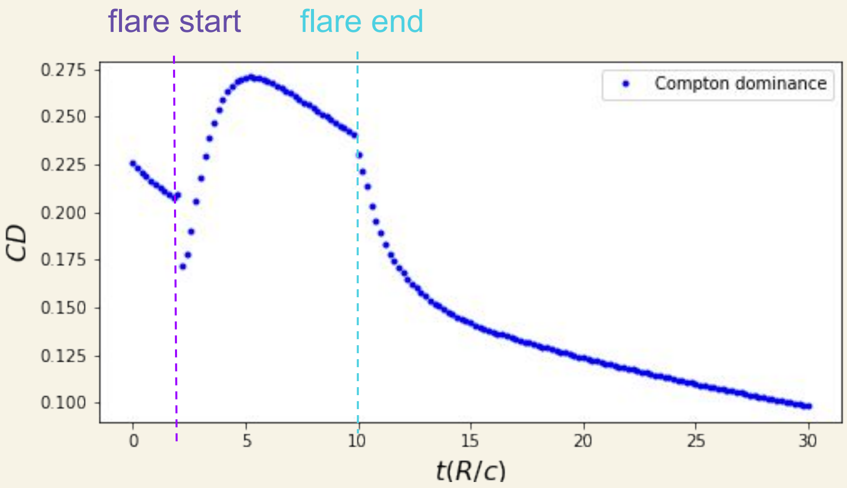

Spectral Energy Distribution

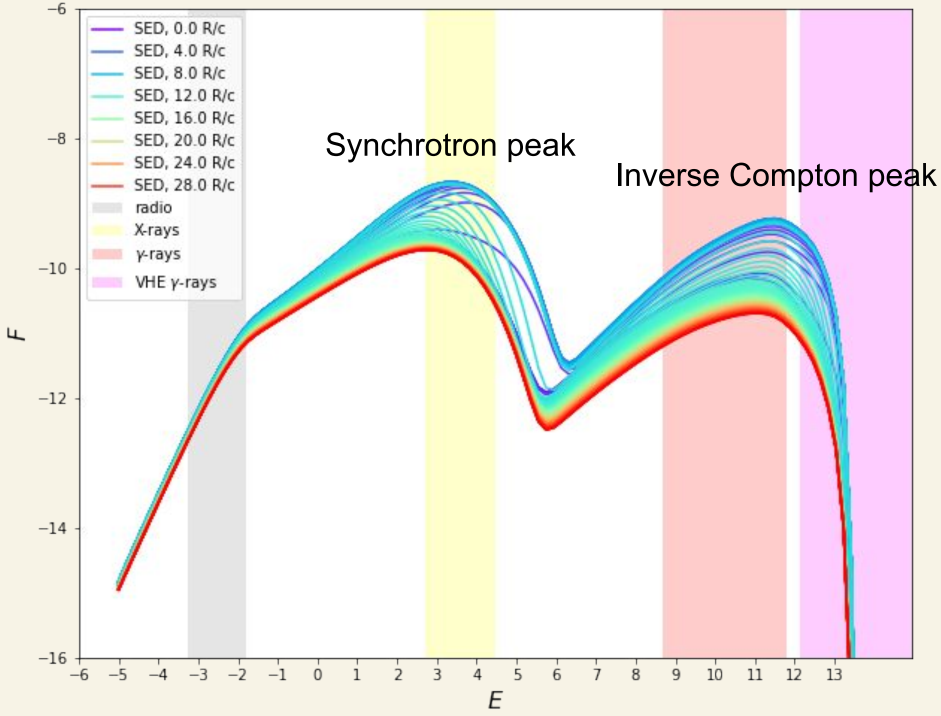

Extra - Fermi II acceleration: hard-sphere regime

Electron Distribution

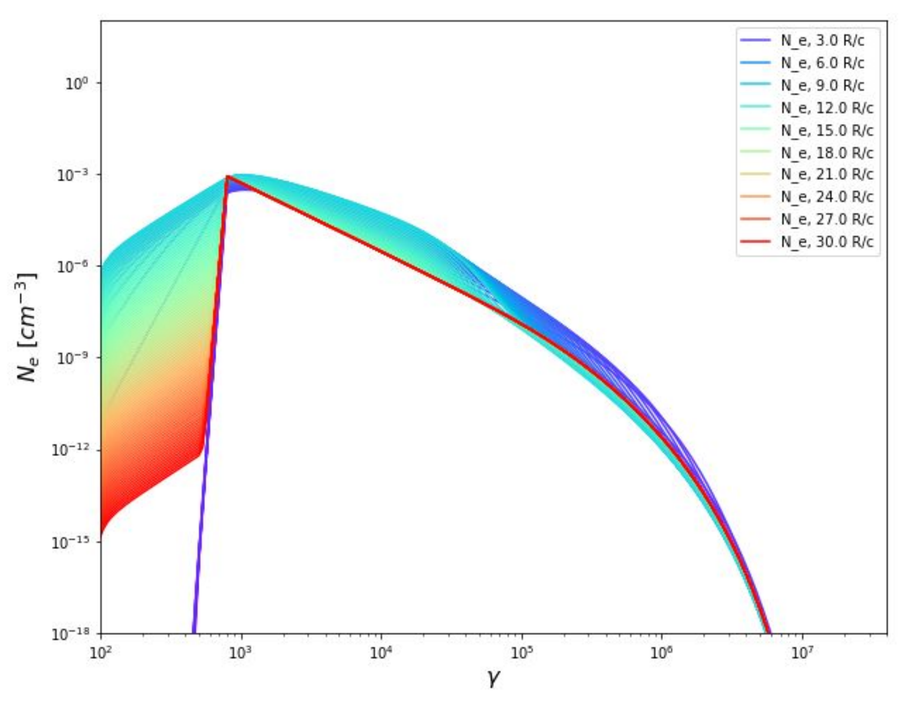

Spectral Energy Distribution (SED)

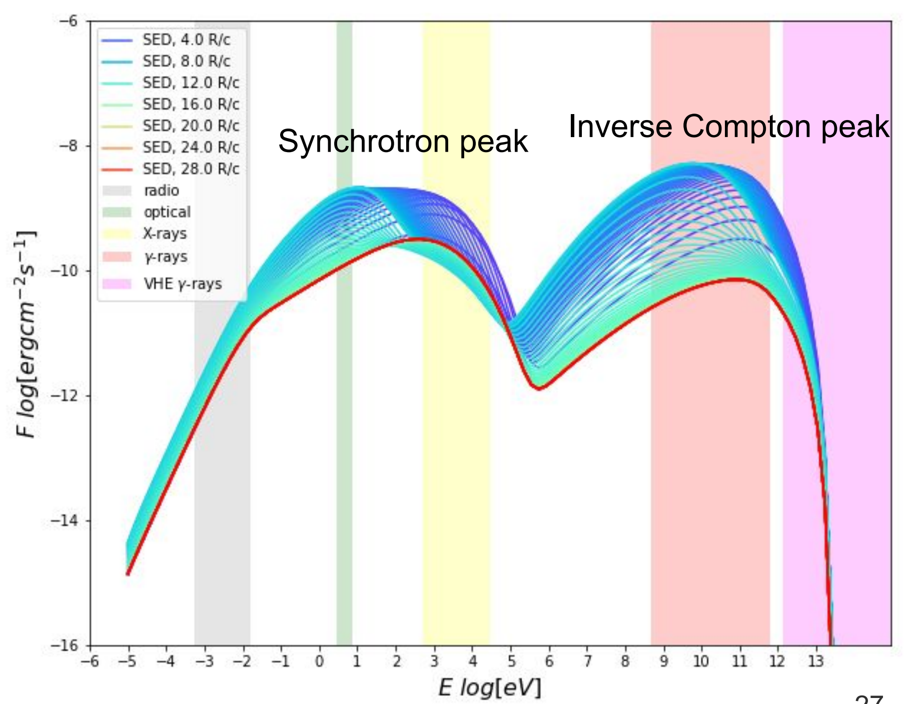

Extra - Fermi II acceleration: hard-sphere regime

Alfvén speed:

$$\beta_A = \frac{1}{\sqrt{1 + \frac{4\mu_0 \epsilon}{3B^2}}}$$

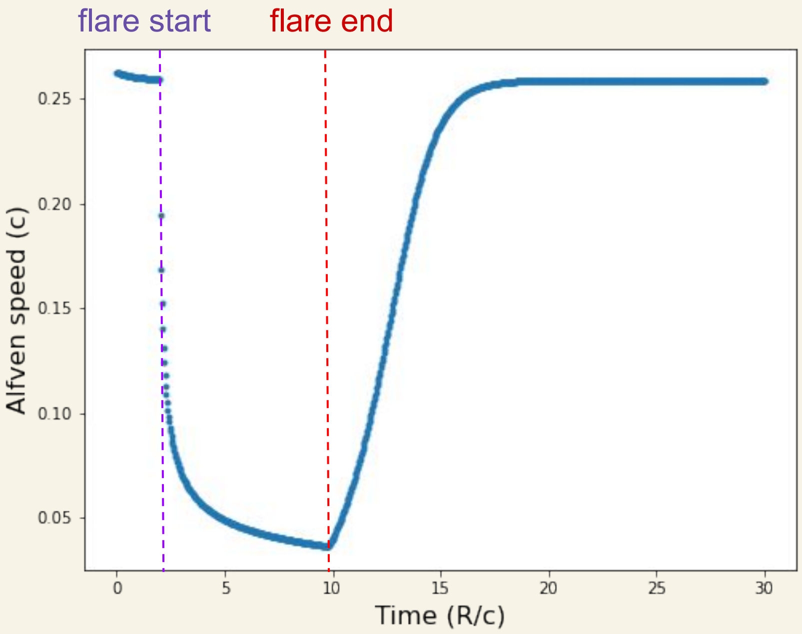

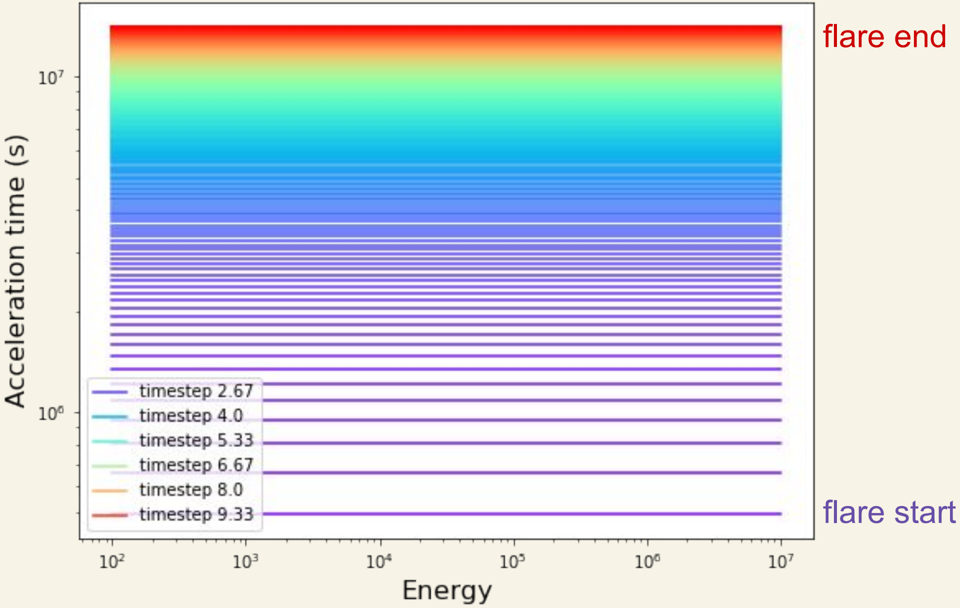

Extra - Fermi II acceleration: hard-sphere regime

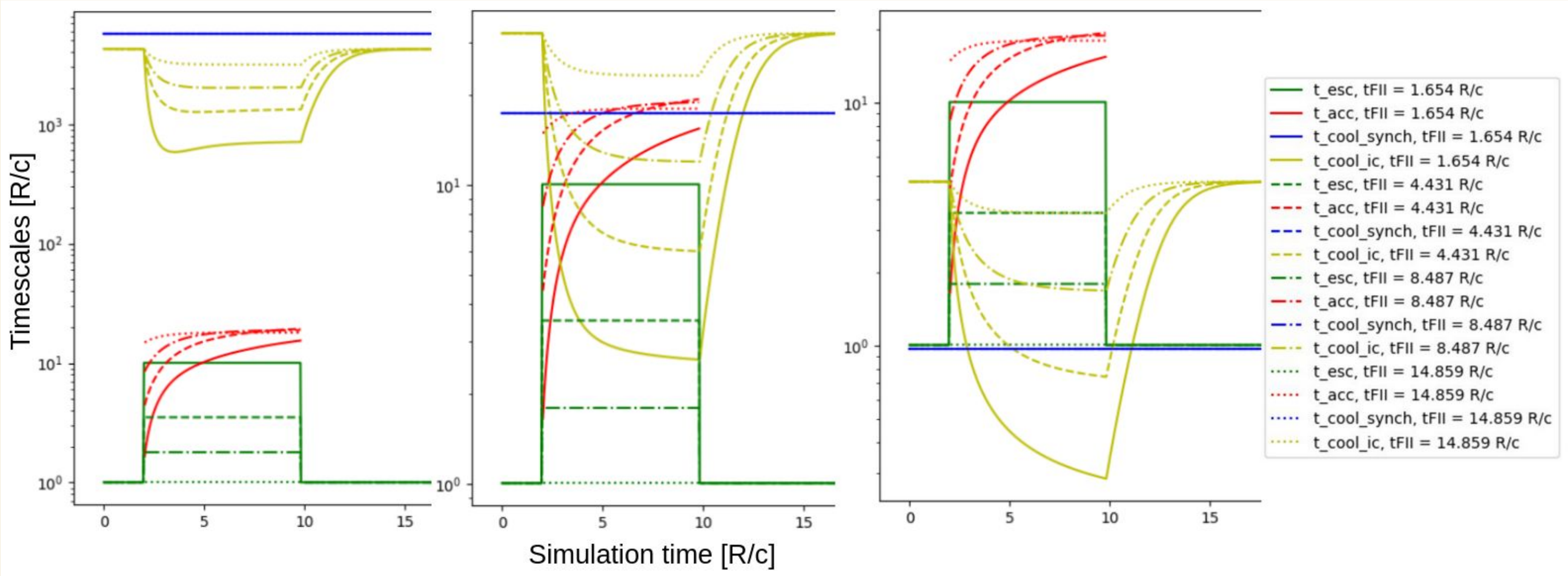

⇒ IC cooling dominates for high energies and short acceleration timescales

Extra - Fermi II acceleration: hard-sphere regime

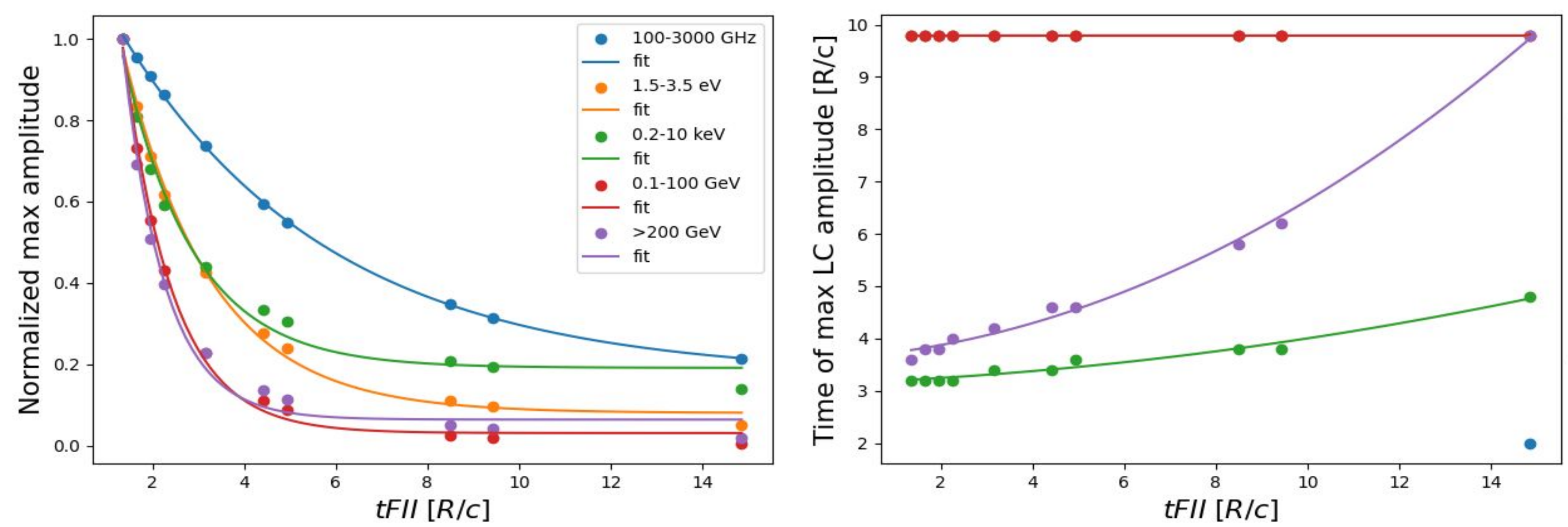

⇒ Known variability amplitude and peak shift behaviour, possible parametrization of the flares

Extra - Fermi II acceleration: Kolmogorov regime

Optical

X-rays

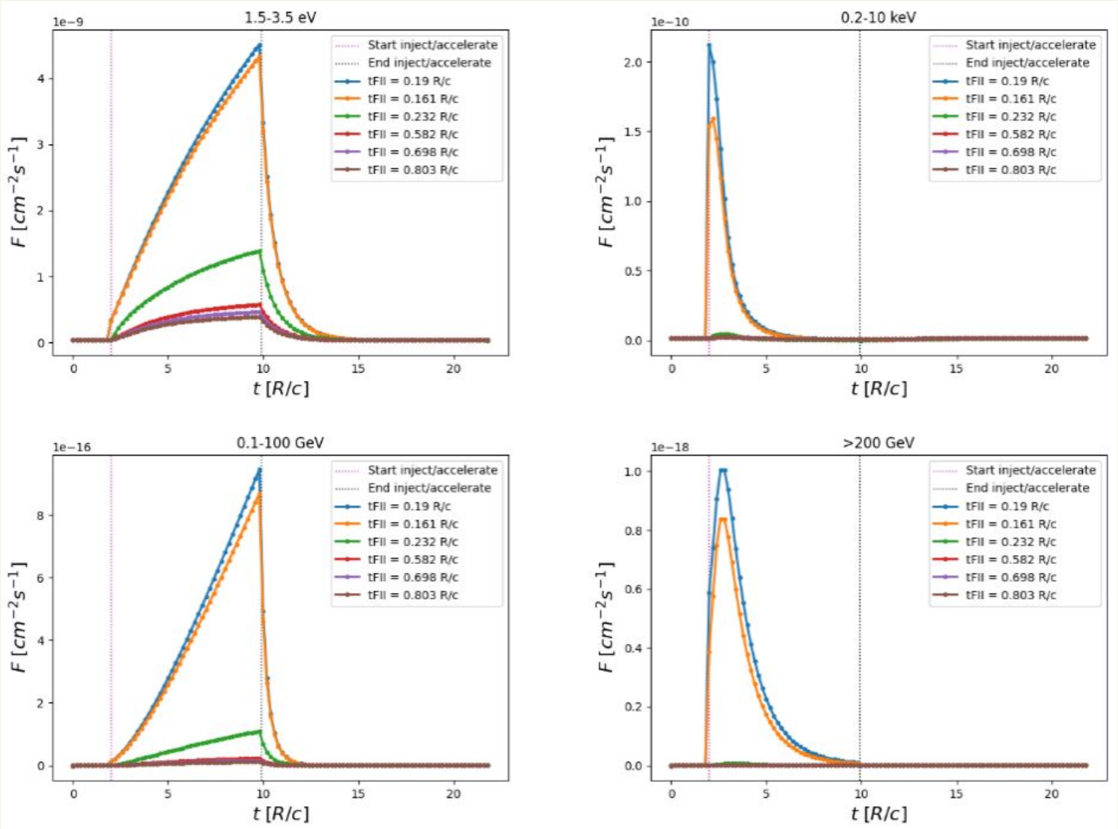

ɣ-rays

VHE ɣ-rays

⇒ Same shapes as high CD hard-sphere turbulence

Extra - Fermi II acceleration: Kraichnan regime

Optical

X-rays

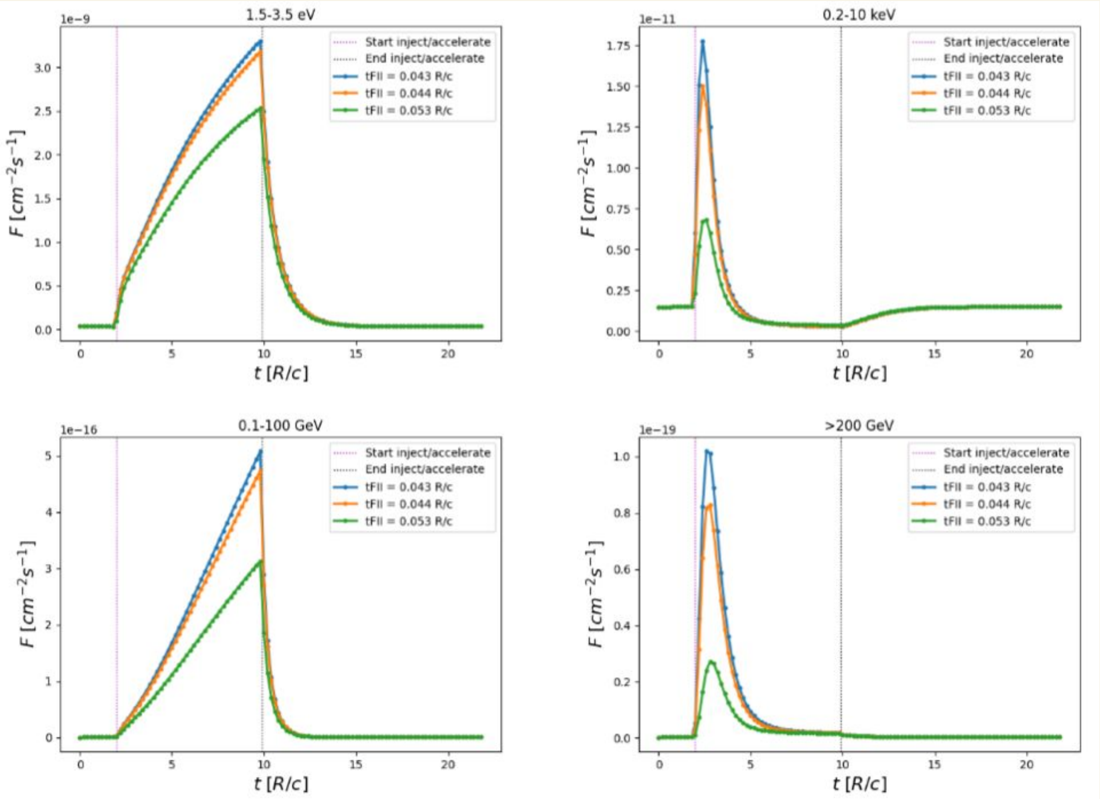

ɣ-rays

VHE ɣ-rays

⇒ Same shapes as high CD hard-sphere turbulence

Extra - Fermi I acceleration

Electron Distribution

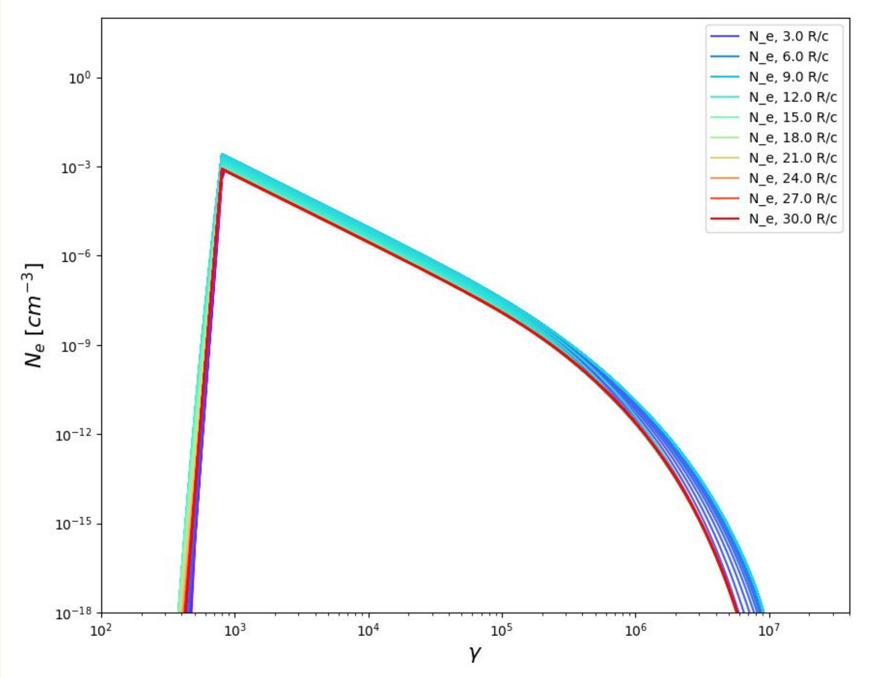

Spectral Energy Distribution (SED)

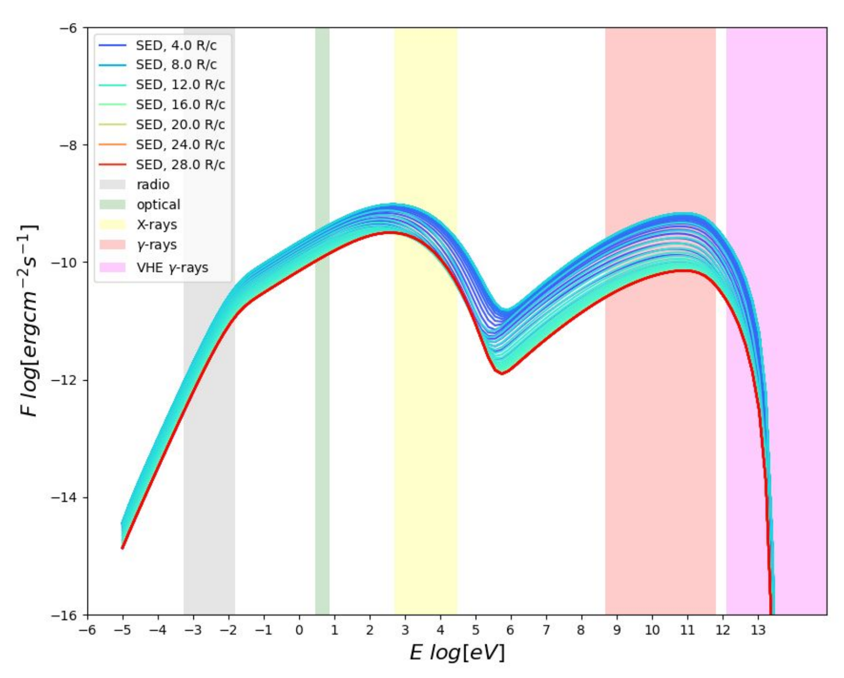

Extra - Fermi I acceleration